Clival chordoma with drop metastases

Faimee Erwan Muhamat Nor[1*], Vijayadwaja Desai[2], Lee Lian Chew[1]

1. Division of Oncologic Imaging, National Cancer Center Singapore, Singapore, Singapore

2. Department of Pathology, Khoo Teck Puat Hospital, Singapore, Singapore

* **Correspondence:** Faimee Erwan Muhamat Nor, Division of Oncologic Imaging, National Cancer Center Singapore, 11 Hospital Drive,
Singapore 169610, Singapore
(✉ *faimee.erwan@yahoo.com*)

ABSTRACT

Chordoma is a rare midline malignant tumor arising from embryonic remnants of the primitive notochord. The base of the skull is the second most common site of disease after the sacrococcygeal region. Intracranial chordoma constitutes about 30-35% of chordoma cases. Metastasis from chordoma is uncommon but if occurs, it tends to spread to the lungs. Cerebrospinal fluid seeding or drop metastasis is very rare. Here we describe a case of a clival chordoma with drop metastases.

CASE REPORT

CASE REPORT

A 59-year-old Chinese lady presented with 2 weeks history of blurred vision. She described a "curtain" obscuring her vision which started in the left eye followed two days later in the right eye. Ophthalmic evaluation revealed bitemporal inferior quadrantanopia.

A magnetic resonance imaging (MRI) of the brain found a lobulated mass in the sellar and suprasellar regions measuring 1.9 x 2.1 x 3.8 cm (anteroposterior x transverse x craniocaudal dimensions) (fig. 1). The mass showed intermediate signal intensity on T1-weighted images and high signal intensity on T2-weighted images. There was homogenous enhancement of the mass on post contrast images. Susceptibility artefacts within the mass were indicative of hemorrhagic foci or calcifications. The optic chiasm was displaced posterolaterally due to mass effect. The mass was closely related to the cavernous sinuses with no evidence of tumor invasion. Areas of abnormal marrow signal with contrast enhancement were noted in the dorsum sellae and clivus on the MRI. Computed tomography (CT) showed a hyperdense sellar/suprasellar mass with irregularity of the dorsum sella turcica and thinning of the sellar floor suggesting erosion (fig. 2). The mass was presumed to be a pituitary macroadenoma, as the normal pituitary gland was not visualized on MRI.

Biochemical tests revealed monomeric hyperprolactinemia, hypocortisolism, hypothyroidism and central diabetes insipidus. A follow-up MRI done a month later showed mild enlargement of the mass, measuring 2.3 x 2.4 x 4.2 cm, with compression of the third ventricle and foramen of Monro (fig. 3). This resulted in acute obstructive hydrocephalus with transependymal cerebrospinal fluid seepage.

The patient thus underwent transphenoidal resection of the mass. Intraoperatively, a well demarcated soft tissue mass was found compressing and flattening the normal pituitary gland anteroinferiorly. The mass was seen spilling into the anterior half of the third ventricle. Gross total resection of the mass was achieved. The Liliequist membrane was intact.

Histopathology demonstrated cellular tissue with cords and nests of physaliferous cells separated by fibrous septa with extensive myxoid stroma (fig. 4). Areas of necrosis were present. No mitotic figures were seen. The tumor cells stained positively with Vimentin, keratins and EMA but stained negatively with synaptophysin. Immunohistochemistry for brachyury to identify notochord differentiation was positive, compatible with chordoma.

Post-operative follow-up imaging showed no residual enhancing tumor in the sella. Staging CT showed no distant metastasis. The patient then underwent adjuvant radiotherapy. About 11 months after surgery, a new small round, homogenously enhancing intradural extramedullary solid nodule was visualized in the anterior foramen magnum,

indenting the medulla oblongata on a surveillance MRI (fig. 5). This lesion showed similar signal characteristics as the index tumor with intermediate signal intensity on T1-weighted images and high signal intensity on T2-weighted images and was deemed to be a drop metastasis. MRI whole spine which was performed to look for other drop metastases found another similar appearing nodular lesion in the posterior epidural space at the L4-5 level (fig. 6), also suspicious for metastasis. The patient was asymptomatic from the metastases and decision was made for expectant management following discussion in a multidisciplinary tumor board and consultation with the patient.

DISCUSSION

Etiology & Demographics:

Chordoma is a rare malignant midline tumor arising from embryonic notochord remnants [1, 2]. It constitutes 1–4% of malignant bone tumors and 0.2–1% of intracranial neoplasms [1, 3, 4]. Intracranial chordomas account for 30-35% of overall chordoma incidence and usually affects the clivus. Clival chordomas are thus very rare tumors. Chordoma peaks at 4th–5th decades of life with male preponderance (2:1) [1, 3, 5].

Clinical & Imaging Findings:

The clinical presentation for patients with intracranial chordomas is dependent on the location of the tumors and occurs in an insidious manner due to the slow-growing nature of the tumor. Generally, they tend to cause diplopia and headache. Abducens nerve tends to be more commonly affected than other cranial nerves. Headaches are usually in the retro-orbital and occipital regions. One may also present with sinonasal congestion if the tumor extends inferiorly into the paranasal sinuses, nasal meati or nasopharynx. Tumors occurring in the sella may compress the pituitary glands and infundibulum, resulting in pituitary dysfunction such as in our case [1, 2].

The classic appearance of intracranial chordoma on CT is that of a centrally located, well-circumscribed, expansile soft-tissue mass that arises from the clivus with associated extensive lytic bone destruction. Chordomas are usually hyperdense to the brain parenchyma on CT [1].

On MRI, chordomas show intermediate to low signal intensity on T1-weighted images [1]. Small foci of T1-weighted hyperintensity can sometimes be visualized in the tumor, representing intratumoral hemorrhage or a mucus pool. Presence of hemorrhage can be confirmed by blooming artefacts on gradient echo images. Classic intracranial chordoma demonstrates high signal intensity on T2-weighted images due to high water content. Contrast enhancement is variable – majority of chordomas show moderate to marked enhancement, however necrotic tumors may have slight or even absent enhancement [1]. Chordomas typically demonstrate calcifications which explain the heterogeneity of these lesions [1, 2]. Calcifications are more frequently found in the mucinous subtypes and are thought to represent bone fragments from adjacent osseous destruction rather than dystrophic calcifications [1]. These are seen as foci of low

signal on T1-weighted and T2-weighted images or abnormal susceptibility artefact on T2* weighted images within the mass on MRI.

MRI is superior to CT for evaluation of chordomas due to excellent soft tissue contrast and multiplanar capabilities. Sagittal images are particularly useful in defining the posterior margin of the tumor, depicting the relation between the tumor and brainstem as well as nasopharyngeal extension of the tumor. Sagittal imaging is also valuable in disclosing transdural transgression, an important factor in surgical planning. The only area in which CT is better than MRI is in evaluation of bony destruction and calcifications [1].

The literature on the evaluation of chordomas using PET imaging is scant and limited to a few case reports that showed chordomas demonstrating hypermetabolism on 18F-FDG PET/CT [6-8].

Treatment & Prognosis:

Chordoma grows slowly but is locally aggressive and associated with high recurrence rate. While it is rarely metastatic, metastases are most commonly to the lungs and in younger patients. Patients with bone metastases have the worst prognosis due to more rapid progression of the disease [4, 9]. Other sites of distant metastasis include the liver, lymph nodes and cerebrospinal fluid seeding. A case of cutaneous metastasis has also been described in the literature [4, 9-12]. Cerebrospinal fluid seeding or drop metastasis is rare because intracranial chordomas are uncommon and they tend to originate at the clivus which is extradural in location [10-14]. Very few cases of spinal dissemination of clival chordoma have been described in the literature [12]. The slow growth rate of chordoma and late age of onset may be masking the true incidence of intradural drop metastases [9]. In addition, a few reported cases of drop metastases were asymptomatic like our case; some cases were discovered only during postmortem examination. Clinically, patients may present with symptoms of lumbago, cauda equina syndrome, paraparesis or sensory disturbances [9, 12].

Dissemination of tumor cells may be caused by the tumor transgressing the dura mater, although tumor spread may also result from surgical intervention [12, 14]. In our case, drop metastases are most likely due to the primary tumor location centered within the dura and disruption of the dura during the surgery.

The metastatic lesions typically have similar imaging appearance to the primary tumor. The bones may be secondarily involved, with scalloping and erosion by the extramedullary lesions [12]. A case report by Uggowitzer et al described drop metastases from a chondroid chordoma which had a dumbbell appearance, mimicking neurogenic tumors [14]. In another case reported by Martin et al, drop metastasis was complicated by an intradural hematoma [9].

Overall median survival time is approximately 6 years with a survival rate of 63-70% at 5 years, falling to 16-51% at 10 years. Prognosis was reported as more favorable in the chondroid subtypes which often feature low grade behavior

compared to the dedifferentiated subtypes which show more aggressive clinical course and features of high grade spindle cell sarcoma [3, 13, 15, 16]. However, Jian BJ et al., in their systematic review of 560 patients who had received treatment for intracranial chordomas, found no significant difference between the prognoses of treated intracranial chondroid chordomas from typical chordomas [16]. Patients with craniocervical lesions show worse prognosis compared to those presenting with lumbosacral lesions [17].

En-bloc surgical resection is the principal treatment for chordomas, even those that involve the cervical spine. There is more favorable prognosis if negative margin is achieved. Aggressive surgical resection shows less than 50% local recurrence rate compared to almost 100% in those with radiotherapy alone or subtotal resections. Surgery can be performed via minimally invasive techniques, e.g. transphenoidal resection or craniotomy. The former may result in inadequate margins due to technical difficulties in clearing the whole tumor [13, 15, 17, 18].

Adjuvant radiotherapy may also be employed to help achieve better long-term outcome particularly in patients with subtotal resections [13, 15, 17, 18]. Radiation doses of more than 60 Gy are usually required to achieve satisfactory treatment. This dosage exceeds the tolerance level of the neurologic structures, particularly the brain stem and optic pathway. Patients undergoing high dose proton radiation have been reported to experience less side effects and can be used in combination with photon therapy [13, 19]. However, a systematic review of 560 patients by Jian BJ et al. showed no significant difference between patients who had surgical resections alone to those coupled with adjuvant radiotherapy [16].

Chordomas, as many other low-grade tumors, are not sensitive to chemotherapy. Thus, the mainstay of the treatment of chordomas lies in achieving negative surgical margins with aggressive primary tumor resection that may be coupled with adjuvant radiotherapy [13, 17].

Differential Diagnoses:
1. Pituitary macroadenoma: This pituitary gland tumour is more than 1 cm in size and may be secreting pituitary hormones, most commonly prolactin. It is slightly hyperdense on CT but will be more hyperdense if complicated by apoplexy. It is isointense on T1-weighted and T2-weighted MRI images with variable contrast enhancement. Cystic change may be seen in some cases but it rarely calcifies [20]. The sella turcica may be scalloped or infiltrated along with the cavernous sinus extension in invasive macroadenoma [21].
2. Perisellar aneurysm: It usually arises from the supraclinoid or cavernous internal carotid arteries. It demonstrates hyperdensity on CT and heterogenous MRI signal. Since it is usually associated with atherosclerosis, rim calcification can be present. It will opacify according to the blood pool unless thrombosed. CT or MR angiogram can be performed to confirm this entity [22].
3. Meningioma: It arises from the arachnoid cells of the inner dura mater. It is a slow growing tumour located most commonly at the sphenoid wings. Typically, it is hyperdense on CT and demonstrates MRI signal akin to gray matter. A third of meningiomas may calcify. Avid contrast enhancement is expected with dural tail and hyperostosis of the underlying bone [23].
4. Plasmacytoma: Extramedullary plasmacytoma usually affects the aerodigestive tract as well as the head and neck region without marrow extension. The larger lesions may show adjacent osseous erosion. Solitary plasmacytoma of the bone may arise in marrow rich clivus and petrous apex with higher tendency to progress into multiple myeloma. The osseous destruction tends to be clean punched out lesions as seen in multiple myeloma with bone expansion in aggressive lesion or solitary bone plasmacytoma. This highly radiosensitive tumour may be accompanied by lymphadenopathy which is usually absent in the case of chordoma [24-26].
5. Chondrosarcoma: A mesenchymal primary skeletal tumour that usually arises from the petro-occipital fissure. Characteristic ring and arc calcifications denoting chondroid matrix will be helpful if present. This heterogeneously enhancing mass may also show more restricted diffusion or higher ADC value than chordoma [27].
6. Ecchordosis physalifora: A benign intradural ectopic notochord remnant mostly found in the prepontine cistern with a stalk attached to the clivus. CT is not ideal for imaging of the posterior fossa due to streak artefacts from the skull base. It is a rare incidental finding on MRI that typically demonstrates T1-weighted hypointensity and T2-weighted hyperintensity. This lesion is considered along the same spectrum as the more aggressive chordoma [28, 29].

TEACHING POINT

Intracranial chordomas are rare but internal calcifications, erosion and marrow involvement of the underlying bones, particularly the clivus, should direct us towards chordoma as a diagnosis. MRI spine should be considered to screen for drop metastases particularly if the primary tumor is located within the dura or has breached the dura.

REFERENCES

1. Erdem E, Angtuaco EC, Van Hemert R, Park JS, Al-Mefty O. Comprehensive review of intracranial chordoma. Radiographics. 2003 Jul-Aug;23(4):995-1009. PMID: 12853676

2. Firooznia H, Pinto RS, Lin JP, Baruch HH, Zausner J. Chordoma: Radiologic evaluation of 20 cases. AJR Am J Roentgenol. 1976 Nov;127(5):797-805. PMID: 973667

3. Hirosawa RM, Santos AB, Fraça MM et al. Intrasellar chondroid chordoma: A case report. ISRN Endocrinol. 2011;2011:259392. PMID: 22500242

4. Young VA, Curtis KM, Temple HT, Eismont FJ, DeLaney TF, Hornicek FJ. Characteristics and Patterns of Metastatic Disease from Chordoma. Sarcoma. 2015;2015:517657. PMID: 26843835

5. Smoll NR, Gautschi OP, Radovanovic I, Schaller K, Weber DC. Incidence and relative survival of chordomas: the standardized mortality ratio and the impact of chordomas on a population. Cancer. 2013 Jun 1;119(11):2029-37. PMID: 23504991

6. Park SA, Kim HS. F-18 FDG PET/CT evaluation of sacrococcygeal chordoma. Clin Nucl Med. 2008 Dec;33(12):906-8. PMID: 19033806

7. Lin CY, Kao CH, Liang JA, Hsieh TC, Yen KY, Sun SS. Chordoma detected on F-18 FDG PET. Clin Nucl Med. 2006 Aug;31(8):506-7. PMID: 16855447

8. Miyazawa N, Ishigame K, Kato S, Satoh Y, Shinohara T. Thoracic chordoma: review and role of FDG-PET. J Neurosurg Sci. 2008 Dec;52(4):117-21; discussion 121-2. Epub 2008 Oct 23. PMID: 18946438

9. Martin MP, Olson S. Intradural drop metastasis of a clival chordoma. J Clin Neurosci. 2009 Aug;16(8):1105-7. doi: 10.1016/j.jocn.2007.11.020. Epub 2009 May 1. PMID: 19410463

10. Goes R, van Overbeeke JJ. A vertebral extra dural chordoma at C5, possibly deriving from a clival chordoma. Surg Neurol Int. 2015 Jun 1;6:94. PMID: 26097773

11. Tamura T, Sato T, Kishida Y et al. Outcome of clival chordomas after skull base surgeries with mean follow-up of 10 years. Fukushima J Med Sci. 2015;61(2):131-40. PMID: 26370681

12. Gala F, Becker AS, Ahmadli U, Pfeiffer M, Kollias S. Extensive Drop Spinal Metastases from Clival Chordoma. Neurographics. 2013 June. Volume 3, Number 2, pp. 87-91(5).

13. Wang HF, Ma HX, Ma CY, Luo YN, Ge PF. Sellar Chordoma Presenting as Pseudo-macroprolactinoma with Unilateral Third Cranial Nerve Palsy. Chin J Cancer Res. 2012 Jun;24(2):167-70. PMID: 23358442

14. Uggowitzer MM, Kugler C, Groell R et al. Drop metastases in a patient with a chondroid chordoma of the clivus. Neuroradiology. 1999 Jul;41(7):504-7. PMID: 10450844

15. Chugh R, Tawbi H, Lucas DR, Biermann JS, Schuetze SM, Baker LH. Chordoma: the nonsarcoma primary bone tumor. Oncologist. 2007 Nov;12(11):1344-50. PMID: 18055855

16. Jian BJ, Bloch OG, Yang I, Han SJ, Aranda D, Parsa AT. A comprehensive analysis of intracranial chordoma and survival: a systematic review. Br J Neurosurg. 2011 Aug;25(4):446-53. PMID: 21749184

17. Yasuda M, Bresson D, Chibbaro S et al. Chordomas of the skull base and cervical spine: clinical outcomes associated with a multimodal surgical resection combined with proton-beam radiation in 40 patients. Neurosurg Rev. 2012 Apr; 35(2):171-82. PMID: 21863225

18. Raffel C, Wright DC, Gutin PH, Wilson CB. Cranial chordomas: clinical presentation and results of operative and radiation therapy in twenty-six patients. Neurosurgery. 1985 Nov;17(5):703-10. PMID: 4069325

19. Rich TA, Schiller A, Suit HD, Mankin HJ. Clinical and pathologic review of 48 cases of chordoma. Cancer. 1985 Jul 1;56(1):182-7. PMID: 2408725

20. Ginsberg LE. Neoplastic diseases affecting the central skull base: CT and MR imaging. AJR Am J Roentgenol. 1992 Sep;159(3):581-9. PMID: 1503031

21. Cottier JP, Destrieux C, Brunereau L et al. Cavernous sinus invasion by pituitary adenoma: MR imaging. Radiology. 2000 May;215(2):463-9. PMID: 10796926

22. Donovan JL, Nesbit GM. Distinction of masses involving the sella and suprasellar space: specificity of imaging features. AJR Am J Roentgenol. 1996 Sep;167(3): 597-603. PMID: 8751659

23. Buetow MP, Buetow PC, Smirniotopoulos JG. Typical, atypical, and misleading features in meningioma. Radiographics. 1991 Nov;11(6):1087-106. PMID: 1749851

24. Wein RO, Popat SR, Doerr TD, Dutcher PO. Plasma cell tumors of the skull base: four case reports and literature review. Skull Base. 2002 May;12(2):77-86. PMID: 17167653

25. Ustuner Z, Basaran M, Kiris T et al. Skull Base Plasmacytoma in a Patient with Light Chain Myeloma. Skull Base. 2003 Aug;13(3):167-171. PMID: 15912174

26. Ooi GC, Chim JC, Au WY, Khong PL. Radiologic manifestations of primary solitary extramedullary and multiple solitary plasmacytomas. AJR Am J Roentgenol. 2006 Mar;186(3):821-7. PMID: 16498114

27. Yeom KW, Lober RM, Mobley BC et al. Diffusion-weighted MRI: distinction of skull base chordoma from chondrosarcoma. AJNR Am J Neuroradiol. 2013 May; 34(5):1056-61. PMID: 23124635

28. Mehnert F, Beschorner R, Küker W, Hahn U, Nägele T. Retroclival ecchordosis physaliphora: MR imaging and review of the literature. AJNR Am J Neuroradiol. 2004 Nov-Dec;25(10):1851-5. PMID: 15569763

29. Ciarpaglini R, Pasquini E, Mazzatenta D, Ambrosini-Spaltro A, Sciarretta V, Frank G. Intradural clival chordoma and ecchordosis physaliphora: a challenging differential diagnosis: case report. Neurosurgery. 2009 Feb;64(2):E387-8. PMID: 19190444
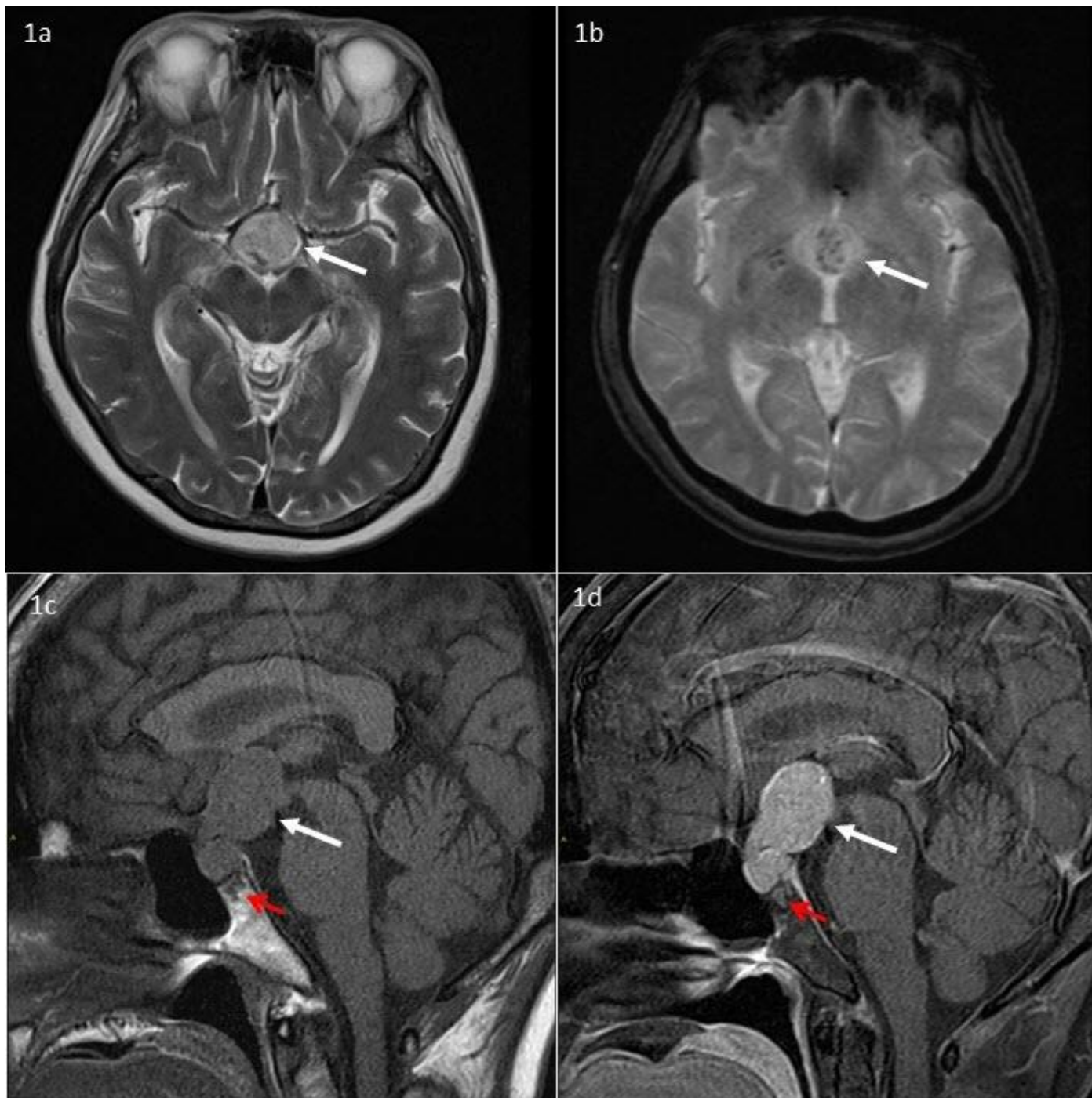
FIGURES

Figure 1: 59-year-old lady with clival chordoma.

Findings: (a) MRI brain shows a lobulated sellar/suprasellar mass with high signal intensity on axial T2W images. (b) Intralesional susceptibility artefacts are suggestive of hemorrhage or calcifications. (c) The tumor is isointense on sagittal pre-contrast T1W sequence with (d) homogenous contrast enhancement. There is also abnormal low T1W signal in the dorsum sellae and superior aspect of the clivus with contrast enhancement (red arrows).

Technique: 1.5T Siemens MAGNETOM Avanto MRI scanner

a) Axial T2W. TR 4350. TE 105. 5mm slice thickness.

b) Axial T2*W. TR 909. TE 26. 5mm slice thickness.

c) Sagittal T1W pre-contrast. TR 400. TE 11. 3mm slice thickness.

d) Sagittal T1W post-contrast. 10ml intravenous Dotarem. TR 540. TE 11. 3mm slice thickness.

Figure 2: 59-year-old lady with clival chordoma.
Findings: (a) Non-contrast axial CT image shows the sellar/suprasellar mass is slightly hyperdense to the brain parenchyma. (b) Sagittal reformatted CT image in the bone window shows mild erosion of the dorsum sellae and thinning of the sellar floor.
Technique: Siemens SOMATOM Definition Flash CT scanner. 120 kV. 67 mAs.
a) Axial soft tissue window. 1mm slice thickness.
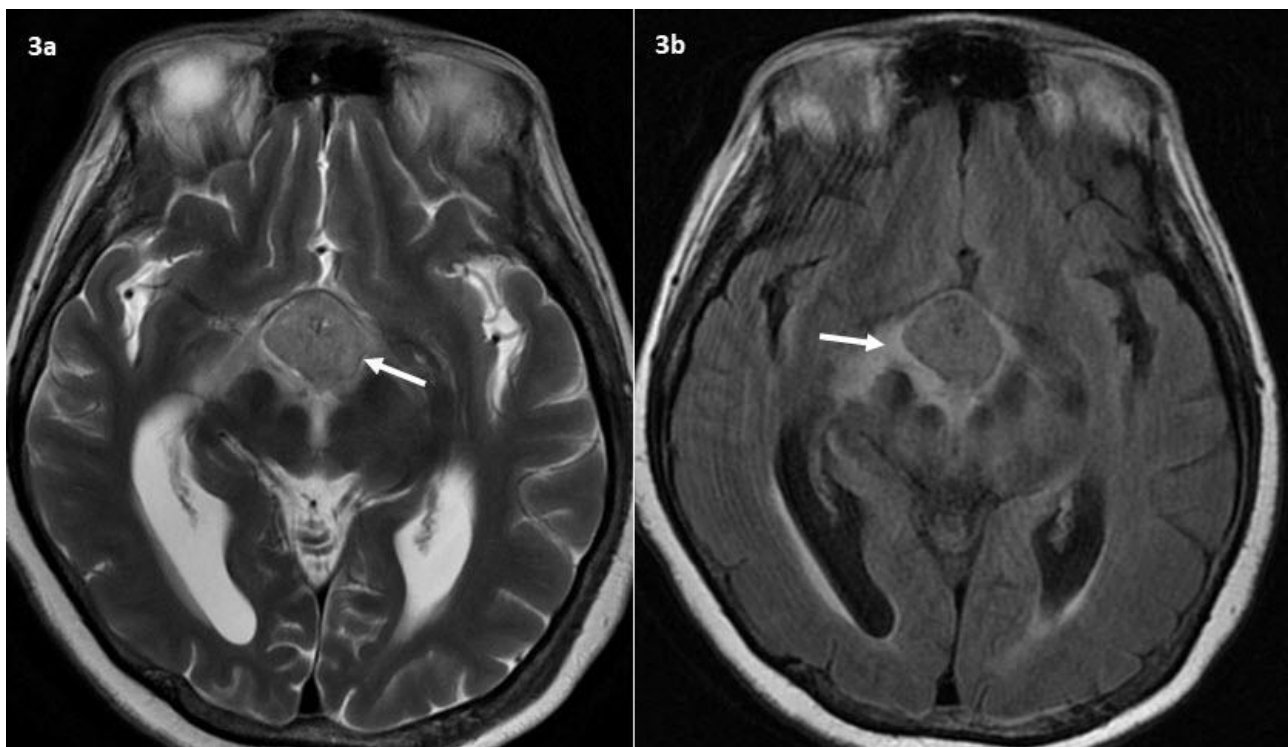b) Sagittal bone window. 3mm slice thickness.

Figure 3: 59-year-old lady with clival chordoma.
Findings: Follow up MRI brain 1 month later. (a) Axial T2W image showed interval enlargement of the sellar/suprasellar mass. (b) Axial T2W FLAIR sequence shows new vasogenic edema around the mass. This is complicated by new acute obstructive hydrocephalus as evidenced by dilatation of the lateral ventricles with cerebrospinal fluid transependymal seepage seen as periventricular high signal.
Technique: 3T General Electric (GE) Discovery MRI scanner
a) Axial T2W. TR 4975. TE 102. 5mm slice thickness.
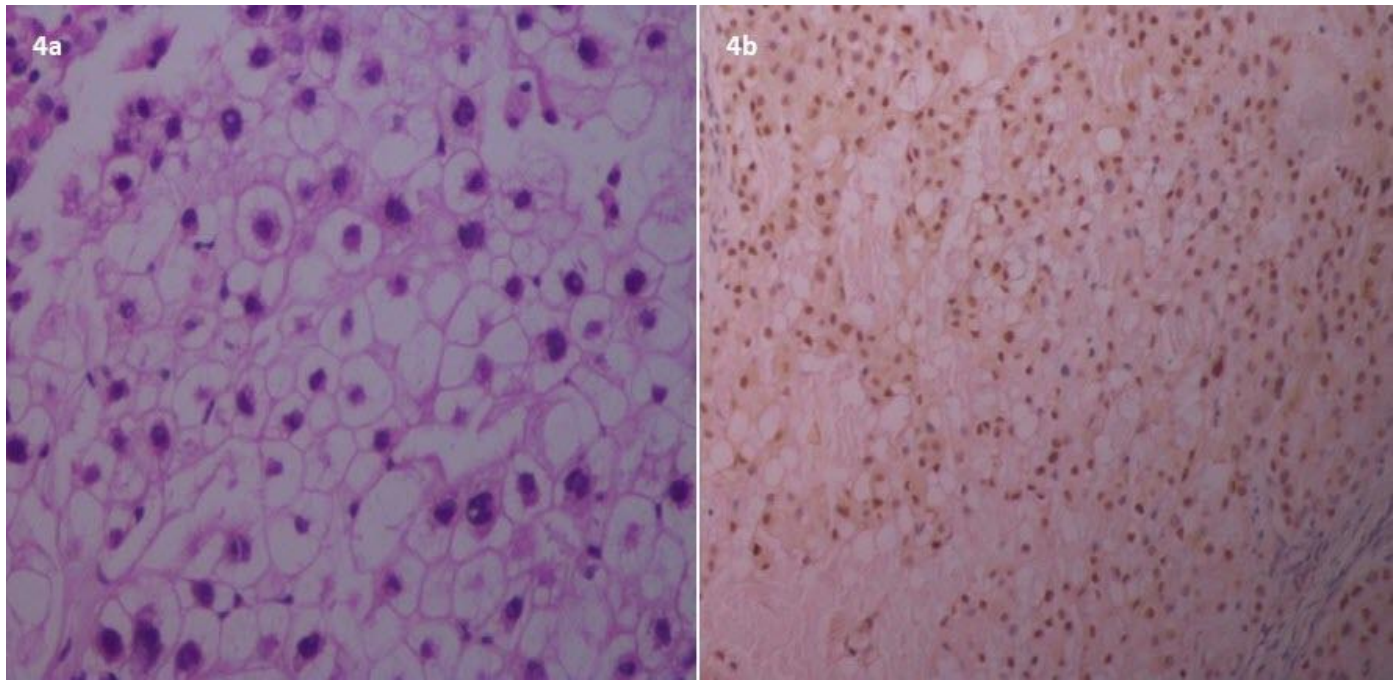b) Axial T2W FLAIR. TR 9000. TE 152. 5mm slice thickness.

Figure 4: 59-year-old lady with clival chordoma.
Findings: Histopathology from the resected sellar/suprasellar mass. (a) Photomicrograph (original magnification, x40; hematoxylin-eosin stain) shows physaliferous cells. The cells have small round nuclei and abundant vacuolated cytoplasm. (b) Tumor cells stain positive with brachyury. Immunohistochemistry is diagnostic of chordoma.
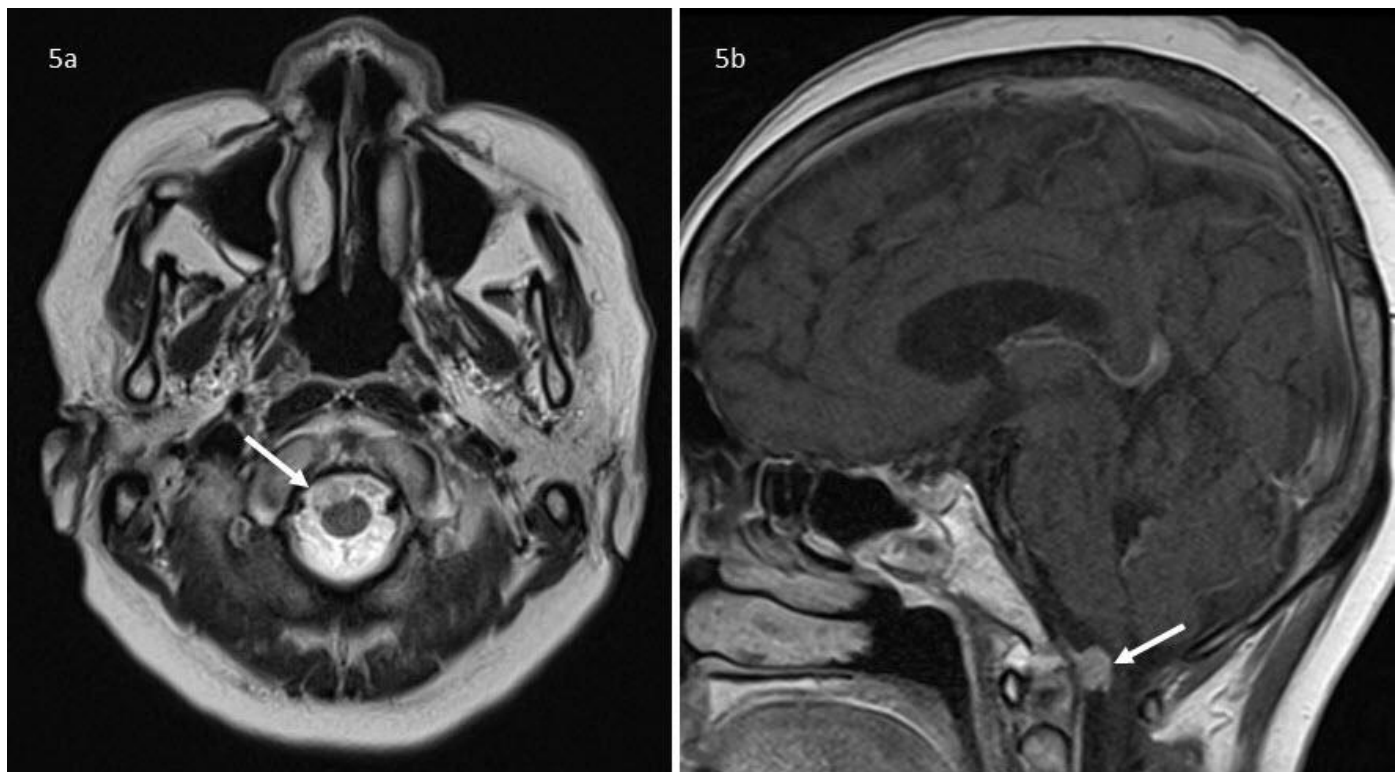

Figure 5: 60-year-old lady with resected clival chordoma about 11 months after the surgery.
Findings: (a) Axial T2W image from surveillance MRI showed a new well circumscribed hyperintense intradural extramedullary nodule at the anterior foramen magnum indenting the medulla. (b) Sagittal post contrast T1W image showed homogenous enhancement of the nodule, suspicious for drop metastasis.
Technique: 1.5T Siemens MAGNETOM Aera MRI scanner
a) Axial T2W. TR 4940. TE 99. 3mm slice thickness.
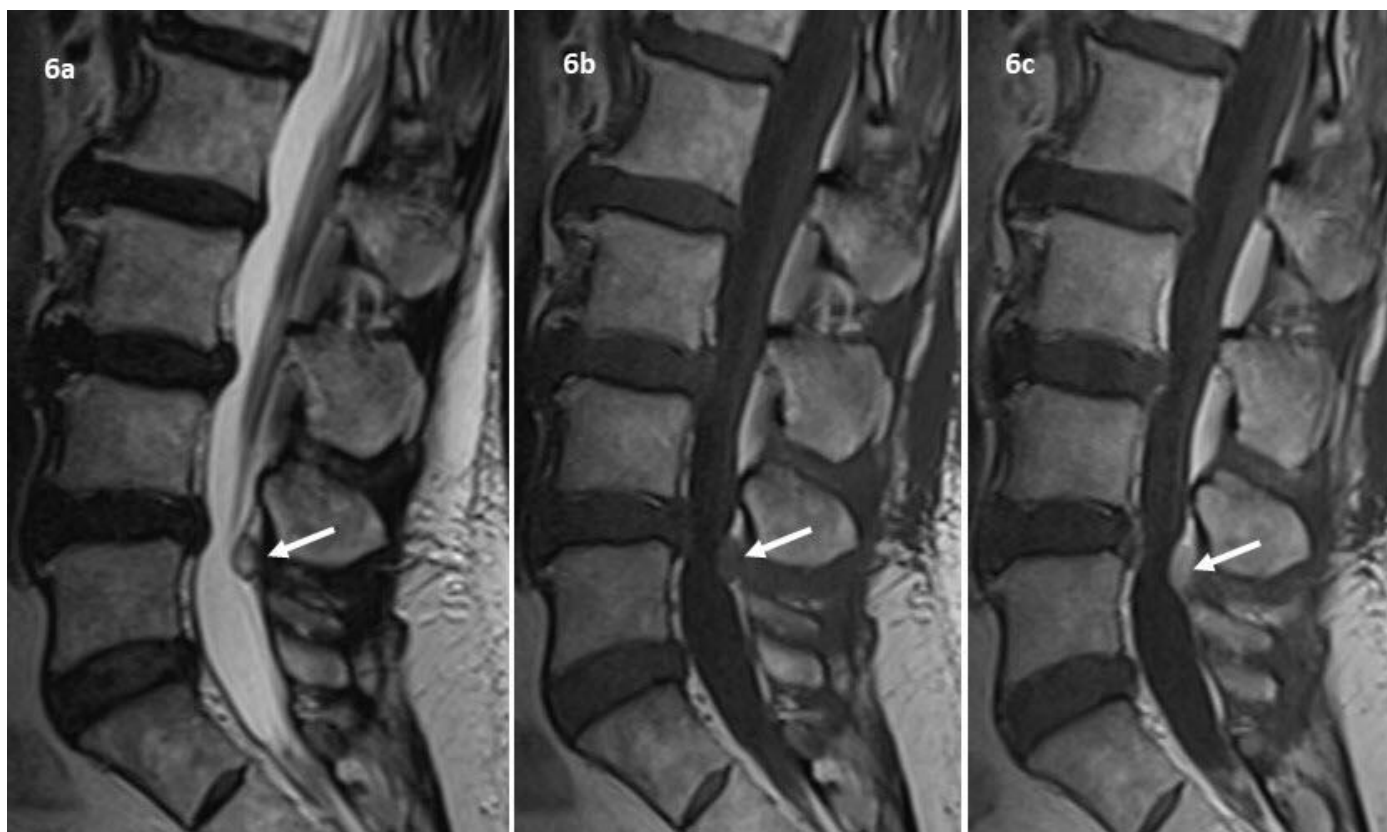b) Sagittal T1W post-contrast. 10ml intravenous Magnevist. TR 531. TE 10. 4mm slice thickness.

Figure 6: 60-year-old lady with resected clival chordoma and new drop metastasis.
Findings: MRI whole spine was done to screen for other drop metastases. (a) Sagittal T2W image showed another well circumscribed hyperintense nodule in the posterior epidural space at the L4-5 level. (b) The nodule is isointense on T1W sequence and (c) demonstrates homogenous contrast enhancement. This was also deemed to be a metastasis as the dura had been breached during the transphenoidal surgery.
Technique: 1.5T Siemens MAGNETOM Aera MRI scanner
a) Sagittal T2W. TR 5000. TE 98. 3mm slice thickness.
b) Sagittal T1W pre-contrast. TR 577. TE 8. 3mm slice thickness.
c) Sagittal T1W post-contrast. 10ml intravenous Dotarem. TR 577. TE 8. 3mm slice thickness.

Etiology	Acquired; arise from notochord remnant
Incidence	Few cases reported
Gender ratio	Male: Female = 2:1
Age predilection	4th-5th decades of life
Risk factors	Unknown
Treatment	Mainly en-bloc surgical resection with or without radiotherapy
Prognosis	Favorable if extradural in location and fully removed surgically. Overall median survival time following treatment is 6 years.
Findings on imaging	Usually, an intracranial chordoma presents as a midline heterogenous soft tissue mass with internal calcifications due to adjacent bone destruction. Most of the time, it involves the clivus. It is hyperdense to brain parenchyma on CT. Intermediate-low T1 signal and high T2 signal are expected on MRI. Blooming artefact on T2* sequence on gradient-echo MRI may be seen, representing haemorrhage or calcifications from the eroded bony fragments. Variable enhancement is seen following intravenous contrast administration. FDG avid on PET.

Table 1: Summary table for sellar/suprasellar chordoma.

Differential diagnosis	Typical location	CT	MRI	18F-FDG PET
Intracranial chordoma	Clivus	Hyperdense enhancing mass with internal calcifications due to adjacent bone erosion.	Enhancing mass that shows mild T1w hypointensity or isointensity with T2w hyperintensity. Calcifications will appear as signal voids or blooming artefact on T2*w sequence.	Hypermetabolic.
Pituitary macroadenoma	Sella	Slightly hyperdense enhancing mass. May be more hyperdense if complicated by apoplexy or hypodense if there is cystic degeneration. Sella turcica may be scalloped. Invasive subtype of pituitary adenomas can erode the bone.	Enhancing mass that shows isointense T1w/T2w signals to gray matter. May be T1w hyperintense if complicated by apoplexy or T1w hypointense/T2w hyperintense if there is cystic degeneration.	Hypermetabolic unless there is cystic degeneration where the cystic area will be hypometabolic.
Perisellar aneurysm	Arising from supraclinoid or cavernous internal carotid arteries	Hyperdense mass with rim calcification and contrast opacification similar to blood pool.	Mass with rim T1w/T2w hypointensity and contrast opacification similar to blood pool.	Similar to blood pool.
Meningioma	Sphenoid wings	Isodense to slightly hyperdense mass with avid contrast enhancement, dural tail and adjacent bone hyperostosis. A third calcifies.	Enhancing mass that shows isointense T1w/T2w signals to gray matter. Avid contrast enhancement, dural tail and adjacent bone hyperostosis.	Hypermetabolic with more avid radiotracer uptake in higher grade tumors.
Plasmacytoma	Aerodigestive tract, head and neck region	Enhancing soft tissue mass with punched-out lytic bone destruction. In advanced disease and solitary bone plasmacytoma, there is also expansion of the affected bones. May have lymphadenopathy.	Enhancing mass with punched-out lytic bone destruction. In advanced disease and solitary bone plasmacytoma, there is also expansion of the affected bones. May have lymphadenopathy.	Hypermetabolic.
Chondrosarcoma	Petro-occipital fissures	Heterogeneously enhancing mass with expansion, bony destruction and endosteal scalloping. Characteristic ring and arc calcifications denote chondroid matrix.	Heterogeneously enhancing mass with mild T1w hypointensity to gray matter and T2w hyperintensity. Calcifications will show susceptibility artefact on T2*w sequence. May show higher ADC value compared to chordoma.	Hypermetabolic with more avid radiotracer uptake in higher grade tumors.
Ecchordosis physalifora	Retroclival, prepontine cistern	Not best modality due to streak artefact in posterior fossa.	Non-enhancing intradural mass with T1w hypointensity and T2w hyperintensity. Stalk attached to clivus.	No literature is available but possibly hypometabolic.

Table 2: Differential diagnosis table for sellar/suprasellar mass.